ORIGINAL RESEARCH

Cerebellocerebral Diaschisis Is the Likely Mechanism of Postsurgical Posterior Fossa Syndrome in Pediatric Patients with Midline Cerebellar Tumors

N.G. Miller
W.E. Reddick
M. Kocak
J.O. Glass
U. Löbel
B. Morris
A. Gajjar
Z. Patay

BACKGROUND AND PURPOSE: PFS occurs in approximately 25% of pediatric patients receiving surgery for midline posterior fossa tumors. Increasing evidence suggests that PFS represents a complex supratentorial cortical dysfunction related to surgery-induced disruption of critical cerebellocerebral connections. The purpose of this study was to determine whether a consistent surgical damage pattern may be identified in patients with PFS by early postoperative anatomic imaging analysis of the pECP and to test whether DSC can detect corresponding changes in cerebral cortical perfusion to indicate a secondary, remote functional disturbance, which could suggest a diaschisis-like pathomechanism.

MATERIALS AND METHODS: Eleven patients with postoperative PFS were evaluated retrospectively and were paired with age- and sex-matched control subjects in whom PFS did not develop. MR imaging work-up included DSC within 3 to 4 weeks after surgery as well as early postoperative anatomic imaging to evaluate components of the pECP.

RESULTS: DSC showed significant decreases in CBF within frontal regions ($P < .05$) and a trend to global cerebral cortical hypoperfusion in patients with PFS. Logistic regression analysis suggested a strong (potentially predictive) relationship between bilateral damage to pECP and the development of PFS ($P = .04$).

CONCLUSIONS: Our data suggest that the primary cause of PFS is the bilateral surgical damage to the pECP. This leads to a trans-synaptic cerebral cortical dysfunction (a form of bilateral crossed cerebellocerebral diaschisis), which manifests with DSC-detectable global, but dominantly frontal, cortical hypoperfusion in patients with patients with PFS compared with age- and sex-matched control subjects.

ABBREVIATIONS: ADC = apparent diffusion coefficient; AIF = arterial input function; CBF = cerebral blood flow; CBV = cerebral blood volume; CCD = cerebellocerebral diaschisis; DSC = dynamic susceptibility-weighted contrast-enhanced perfusion MR imaging; FLAIR = fluid-attenuated inversion recovery; GBCA = gadolinium-based contrast agent; PD = proton-attenuation; pECP = proximal efferent cerebellar pathway; PFS = posterior fossa syndrome; ROIs = regions of interest.

PFS is a devastating complication of surgery encountered in patients operated on for midline tumors in the posterior fossa. It develops in approximately 25% of pediatric patients undergoing posterior fossa surgery and is characterized by a profound neuropsychological disturbance, the central manifestation of which is cerebellar mutism.[1] Although most patients show some improvement with time, many of them do not fully recover. The impact of PFS on patients, families, and health care providers is considerable.

In the past, several different conditions have been advocated to be associated with the development of PFS, including brain stem compression, hydrocephalus, and damage to the inferior cerebellar vermis.[1,2] On the basis of a single case observation, it has also been hypothesized that the development of PFS requires bilateral damage to the dentate nuclei and/or its outflow tract, the efferent cerebellar pathway, during surgery.[3,4] Although this hypothesis has not yet been confirmed in larger-scale studies, it is quite conceivable because proximal components (dentate nuclei, superior cerebellar peduncles, and their decussation in the mesencephalic tegmentum) of the efferent cerebellar pathway are often invaded by posterior fossa tumors and are prone to surgical damage from radical resection. Efferent fibers from the dentate nuclei leave the cerebellum through the superior cerebellar peduncle, decussate in the mesencephalic tegmentum, and synapse in the ventral lateral/ventral anterior nuclei of the thalamus.[5] The corresponding postsynaptic neurons project to widespread cortical areas, including the primary motor, premotor, and prefrontal cortex.[5] Therefore, theoretically, bilateral damage to the pECP has the potential to disrupt the efferent cerebellar signals and deprive the cerebral cortex of cerebellar input in a fairly global fashion. Considering the function of the above-mentioned cortical areas (movement; movement coordination; and executive functioning, respectively), a functional disconnection of these areas may cause a complex neuropsychologi-

Received March 13, 2009; accepted after revision July 8.

From the Departments of Radiological Sciences (N.G.M., W.E.R., J.O.G., U.L., Z.P.), Biostatistics (M.K.), and Oncology (B.M., A.G.), St. Jude Children's Research Hospital, Memphis, Tennessee.

This work was supported in part by Cancer Center Support grant P30-CA21765 from the National Cancer Institute and by the American Lebanese Syrian Associated Charities.

Previously presented in 2 parts at: Annual Meeting of the American Society of Neuroradiology, Vancouver, British Columbia, Canada, May 16–21, 2009.

Please address correspondence to Zoltan Patay, St. Jude Children's Research Hostpital, 262 Danny Thomas Pl, Memphis, TN 38105; e-mail: zoltan.patay@stjude.org

DOI 10.3174/ajnr.A1821

cal disturbance, such as PFS, with significant impact on various aspects of neurocognition. This would imply that PFS is a complex functional disturbance, affecting cortical areas involved in critical neurocognitive processes,[6] which develops remotely from the site of surgical injury through a trans-synaptic "reflex" mechanism. All of these ideas raise the possibility of diaschisis being the likely pathomechanism of these phenomena.

Diaschisis is traditionally defined as sudden inhibition of function in an area of the brain remote, but anatomically connected through trans-synaptic neural pathways, to the site of primary injury. The most common form of diaschisis is crossed cerebrocerebellar diaschisis, which has been extensively investigated by nuclear medicine techniques. The hallmark features of diaschisis are hypoperfusion, decreased oxygen consumption, and hypometabolism. DSC has been shown to be a robust technique to quantitatively evaluate brain perfusion. It provides important hemodynamic parameters such as CBF and CBV, mean transit time, and time-to-peak. In a small cohort of patients with large cerebral infarctions, investigators have been able to show measurable perfusion changes within the contralateral cerebellar cortex by using this technique, confirming the feasibility of in vivo measurement of diaschisis-related perfusion changes in humans.[7]

Taking into account all available literature data and our own clinical experience, the purpose of our study was to identify and describe the missing link between an apparent surgical cause in the posterior fossa and the resultant clinical manifestations pointing to a remote, supratentorial functional disturbance and also to propose a plausible pathomechanism of PFS. In this retrospective but hypothesis-driven study, we sought to establish the relationship between patterns of surgical damage to the pECP and the onset of PFS through postoperative anatomic damage analysis, as well as to determine whether DSC-detectable changes in cerebral cortical perfusion occur in patients with PFS compared with control subjects, which would indicate a secondary functional disturbance through a diaschisis-like pathomechanism.

Materials and Methods

Subjects

This study was designed as a retrospective case-control study comparing patients who had PFS after posterior fossa surgery with patients who also received surgery but did not go on to have PFS. All patients enrolled in the study came from an ongoing institutional review board–approved clinical research protocol carried out at our institution involving children diagnosed with posterior fossa medulloblastoma, atypical teratoid-rhabdoid tumor, or primitive neuroectodermal tumors. Per the research protocol, treatment of these patients includes maximal surgical resection, craniospinal radiation therapy, and chemotherapy. Informed consent was obtained from these patients and their families on enrollment in the protocol.

The criterion for primary inclusion in our study was the development of PFS after surgery. Because this was a retrospective study and most of the PFS cases were diagnosed at outside institutions before referral to our hospital, we were unable to standardize the diagnostic criteria or obtain exact PFS diagnosis dates. However, we found 18 patients from the past 5 years who were diagnosed with PFS within 1 week after surgery. Once enrolled in our protocol, all further MR imaging follow-ups were performed at our institution according to protocol requirements. The MR imaging protocol includes DSC in every patient at similar time points during the treatment and posttreatment follow-up periods, which provided us with the necessary raw data for all patients (PFS cases and control subjects) selected for our study.

The DSC scans of these patients were initially screened to ensure that there were no artifacts affecting the overall quality of the data and that adequate data were collected from the supratentorial compartment. After the initial screening, 3 patients with PFS were removed from the study because of metal artifacts from ventriculoperitoneal shunts, and 3 more patients were removed because perfusion data were either not acquired or not acquired as dictated by standard protocol requirements. Overall, 12 patients with PFS were retained for our study.

For each of these 12 patients, another patient from among those enrolled in the same protocol in whom PFS did not develop after surgery, of the same sex and closest in age at the time of data collection, was selected as a matched control. Age and sex matching were performed because literature data suggest that blood perfusion may differ depending on the age and sex of the patient.[8,9] During the course of the study, we discovered that one of the patients underwent posterior fossa surgery on 2 occasions. We excluded this patient and the corresponding control subject because we were unable to confirm whether the first or second surgery caused the development of PFS. Thus, information from 11 PFS case patients and control subjects was included in our study. Ages of the PFS patient group ranged from 3.33 to 10.88 years, with a mean of 7.10 years. Ages of the control patient group ranged from 3.19 to 10.64 years, with a mean of 7.33 years.

Anatomic Data Collection

We performed a conventional analysis of the postoperative integrity of key structures in the pECP of each patient using axial and coronal T2-weighted, axial diffusion-weighted, and, occasionally, other anatomic image types as available or needed. As most of these surgeries were performed at outside institutions, not all image sequences were available for analysis on every patient. This was a blind analysis performed by a neuroradiologist. Each patient received a damage value of 0 to 3 for 6 structures representing the pECP (left and right dentate nuclei, left and right superior cerebellar peduncle, and left and right pontomesencephalic tegmentum). The damage value indicates the integrity of each structure in the following way: a damage value of "0" indicated no damage, "1" indicated signal intensity and morphologic changes suggesting surgery-induced vasogenic edema without obvious structural damage, "2" indicated possible or partial structural damage, and "3" indicated definite tissue damage. Definite tissue damage was presumed when there was obvious structural damage (eg, trans-section of superior cerebellar peduncle, resection of dentate nucleus) to any of the index anatomic entities or when diffusion data (such as restricted water diffusion, indicating cytotoxic edema) suggested profound, likely irreversible "functional" changes at the cellular level within a given structure. Following this initial data collection, information from each of the 6 structures was condensed to determine whether there was left- and/or right-sided damage to the key components of the pECP for each patient. If a patient had a value of 3 for any of the structures on the left side, we indicated that the integrity of the entire left pECP was damaged. Conversely, a value of 3 for any structures on the right side indicated global functional damage to the right pECP. We then assigned the patients into 3 groups on the basis of anatomic damage: no damage, unilateral damage, and bilateral damage to the pECP.

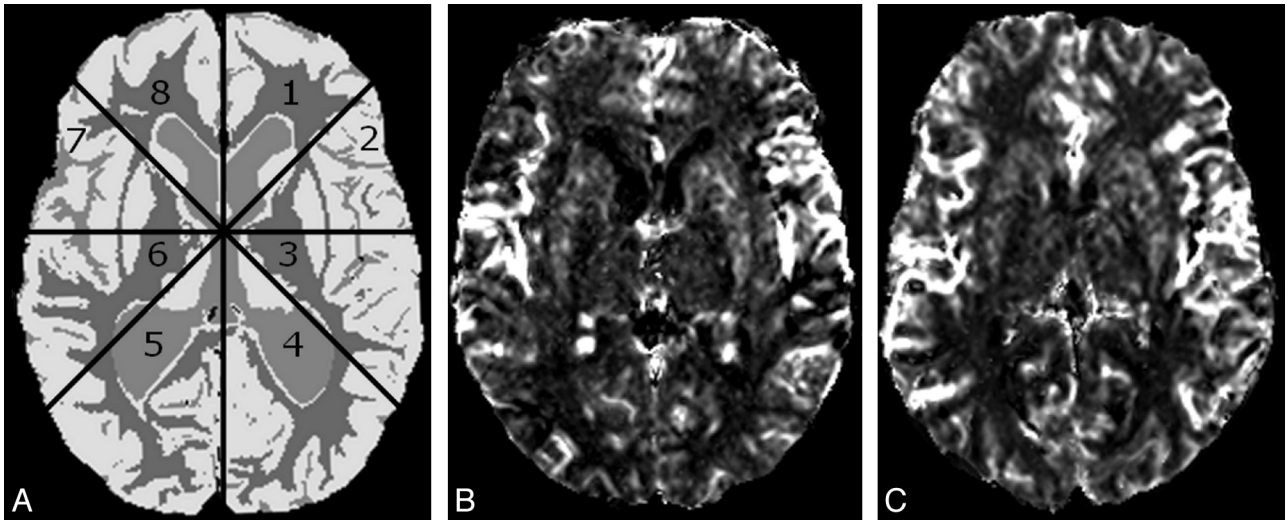

Fig 1. Example of segmentation of gray and white matter and definition of subvolumes 1 to 8 for section 5 (*A*). The segmentation map (*A*) was overlaid on corresponding CBV and CBF parametric maps of patients with PFS and control subjects (image *B* is a CBF map of a patient with PFS, and image *C* is that of a matched control subject).

Perfusion Data Collection

All patients received clinical MR imaging scans (1.5T Avanto scanner; Siemens, Erlangen, Germany) consisting of T1-, T2-, and PD images; FLAIR; and contrast-enhanced T1-weighted scans covering the entire brain. In addition, echo-planar diffusion-weighted imaging was performed ($b = 1000$). DSC data were acquired during bolus intravenous injection of a GBCA (Omniscan or Magnevist; Bayer HealthCare Pharmaceuticals, Wayne, New Jersey) through a 22-G intravenous line at a rate of 0.8 to 1.0 mL/s delivered by a power injector. We used the regular dose (0.2 mL/kg); hence, the total amount of the injected GBCA was a function of the patient's body weight. The actual injected volumes ranged between 2 and 12.5 mL (mean, 5 mL) for the control group and 3 to 10 mL (mean, 5 mL) for patients with PFS. The total injection times ranged between 2 to 13 s (n.b. these injection rates of 0.8–1.0 mL/s were imposed by institutional policy/protocol requirements).

The DSC sequence used in our patients was an echo-planar–based multisection 2D acquisition (TR, 1910 ms; TE, 50 ms, NEX, 1; bandwidth, 1346/pixel; FOV, 210 mm; matrix size, 128 × 128 with a partial Fourier factor of 7/8; number of sections, 15; section thickness, 5 mm with no gap; number of measurements per section, 50). The acquisition started approximately 35–40 s before the contrast arrival to the intracranial space and ended after a few recirculation passes of contrast, with the first pass roughly in the middle of the acquisition.

DSC data analysis was performed for a stack of seven 5-mm-thick contiguous transverse sections covering the supratentorial compartment. The most caudal section in which both the genu and the splenium of the corpus callosum could be visualized was assigned as the index section, and data were analyzed for that section as well as 4 sections rostral and 2 sections caudal.

Each conventional image set (T1/PD/FLAIR) was registered to the T2-weighted set, and the intensity inhomogeneity on the MR images was corrected with use of a new implementation of an entropy-minimization algorithm.[10] Tissues within the brain parenchyma were segmented with an automated hybrid neural network segmentation and classification method.[11] The resulting classified regions were mapped to a color scheme delineating gray matter, white matter, and CSF. Robust reliability and validity have been established for these methods, resulting in a predicted variance of approximately 2% in the repeated measures of white and gray matter volumes.[12]

Processing of the perfusion imaging dataset to determine the brain hemodynamic parameters was achieved through an iterative process by use of the Kohonen self-organizing map for a robust automatic identification of normalized AIF.[13] Once the AIF was obtained, a nonparametric deconvolution of the tissue signal intensity with AIF and leakage correction models was used to create parametric images of CBV and CBF for all sections in the DSC image set. These parametric maps were then affine registered to the color image set used for the tissue volume analysis.

We arbitrarily divided the global volume of interest (defined as the sum of the 7 DSC sections) into 8 equal ($\pi/4$) subvolumes to investigate regional perfusion changes in cortical gray matter. The first division was by hemisphere. Each hemisphere was then divided into 4 regions: frontal-polar, frontal, temporoparietal, and parieto-occipital. We created these subvolumes of interest automatically by computer using the above-detailed parcellation scheme. We manually selected ROIs on all sections of the segmented tissue color maps that corresponded with deep gray matter structures (both putamina, caudate nuclei, and thalami). Because the parametric perfusion maps were registered to the segmented tissue color maps, we used these ROIs to obtain perfusion data for these structures. We also manually excluded the deep gray matter structures from the acquisition of cortical perfusion data.

For each section, we acquired perfusion data by calculating the mean CBF (mL/min/100 g) and CBV (% of total volume) for each of the deep gray matter structures as well as from the cortical gray matter in the 8 regions described previously (Fig. 1). Use of the local AIF allowed for absolute quantification of CBF and CBV as a percentage of the voxel volume. After collection of the data by section, information for each of the 7 sections was incorporated to provide aggregate values of CBF and CBV for each of the 8 cortical regions as well as aggregate values for each of the deep gray matter structures.

Statistical Analysis

Logistic regression was used to investigate whether unilateral or bilateral surgical damage to the pECP visualized by conventional and diffusion-weighted MR imaging can be used to predict the development of PFS on early postoperative imaging studies. For the perfusion analysis, PFS case patients and control subjects were compared in CBF and CBV at the aggregate and section level by region with the Wilcoxon

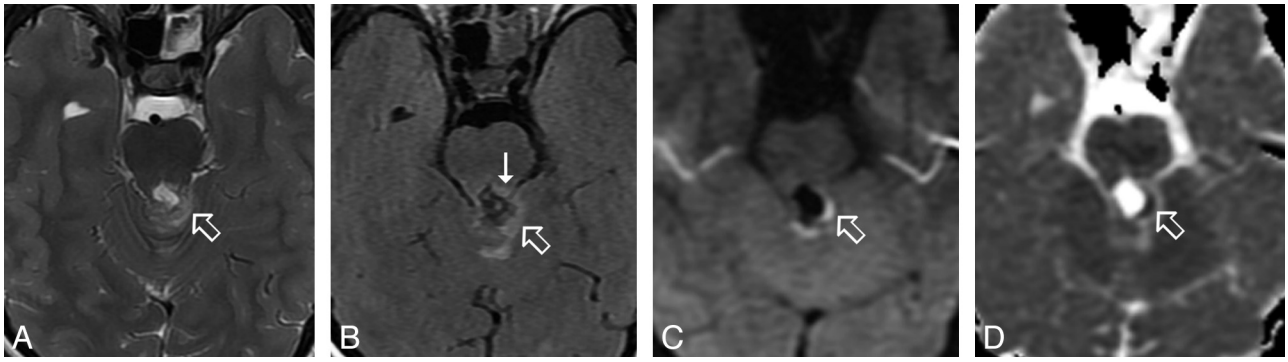

Fig 2. Axial T2-weighted (*A*), FLAIR (*B*), diffusion-weighted (*C*), and ADC map (*D*) images demonstrating surgical damage to the upper portion of the left superior cerebellar peduncle (*open arrow*) and the mesencephalic tegmentum (*solid arrow*). Diffusion-weighted and ADC map images show restricted water diffusion, consistent with cytotoxic edema. This finding was interpreted as permanent damage to the left superior cerebellar peduncle.

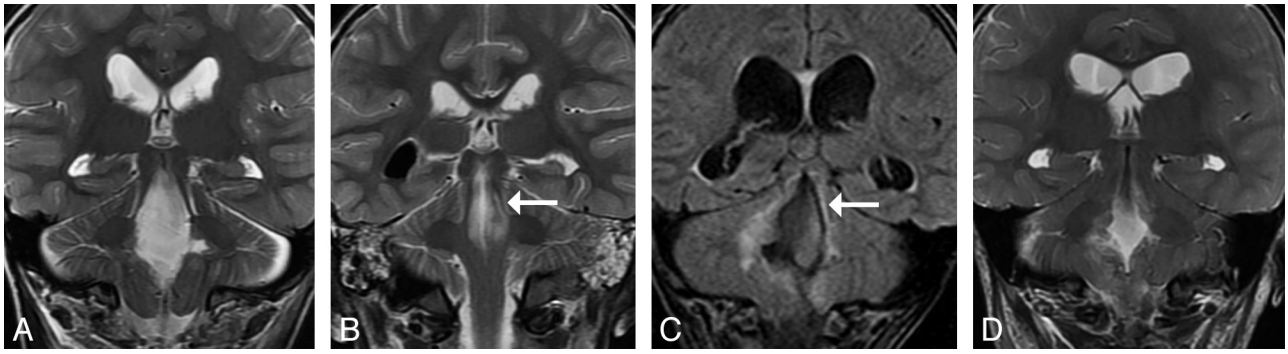

Fig 3. Coronal T2-weighted (*A,B,D*) and FLAIR (*C*) images demonstrating no damage (*A*), unilateral damage (*B,C*), and bilateral damage (*D*) to the superior cerebellar peduncles in 4 different patients. On image *B*, it is uncertain whether the signal intensity and structural changes (*arrow*) represent complete damage or correspond to postsurgical edema only (patient did not have PFS). On image *C*, damage to the right superior cerebellar peduncle (and dentate nucleus) is unequivocal, whereas hypersignal on the left side (*arrow*) may be interpreted as postsurgical edema (patient had PFS; damaged left dentate nucleus not shown).

signed rank test. Because this was an exploratory study, we wanted to be certain that our analyses were sensitive enough to detect any potential differences between PFS case patients and control subjects. Therefore, *P* values resulting from these analyses were not adjusted for multiplicity. All statistical tests were performed with the level of significance set at the $P = .05$ level.

Results

Anatomic Damage Analysis

Anatomic imaging suggested bilateral damage to the pECP in 7 patients, 6 of whom actually went on to have PFS. A total of 15 patients had apparent unilateral damage, and only 5 of them had PFS. Figures 2–5 illustrate examples of cases with varying damage patterns within the pECP. The logistic regression analysis showed that the point estimate of the odds ratio was 12 (95% confidence interval, 1.12–129), which suggests that one has a better-than-random chance to predict the onset of PFS on the basis of the analysis of surgical damage by using conventional MR images ($P = .04$).

Perfusion Data Analysis

Average aggregate values of CBF in the 8 cortical regions over the 7 contiguous sections ranged from 65.3 to 97.6 mL/min/100 g for the control patients and from 53.5 to 86.5 mL/min/100 g for the patients with PFS. For the same regions, average aggregate values of CBV ranged from 8.25% to 10.34% in various regions for the control patients and from 7.50% to 9.51% for the patients with PFS. In fact, aggregate CBF and CBV were lower in every region for patients with PFS compared with control subjects. There seems to be a consistent, statistically significant difference in CBF within the right frontal region, with patients with PFS hypoperfused compared with control patients ($P < .05$). There were also significant CBF decreases for patients with PFS within areas of the left frontal region, right temporal parietal region, and left and right frontal polar regions ($P < .05$). Average values for CBF in deep gray matter structures ranged from 55.9 to 67.6 mL/min/100 g in control subjects and from 47.3 to 54.5 mL/min/100 g in patients with PFS. CBV in deep gray matter structures ranged from 6.07% to 9.20% in control subjects and from 5.40% to 8.44% in patients with PFS. A description of areas of significant difference with corresponding *P* values is provided in the accompanying Table.

Discussion

Other investigators have already attributed the development of PFS to bilateral damage of the dentate nuclei or its projections during surgery.[3,4] With medulloblastomas frequently exhibiting multidirectional invasive growth, including either isolated or combined involvement of key components of the pECP, attempts to achieve gross total tumor resection carry a significant risk for such collateral damage. Building on these concepts, we speculated that PFS may be the result of bilateral damage anywhere along the pECP. This would mean that

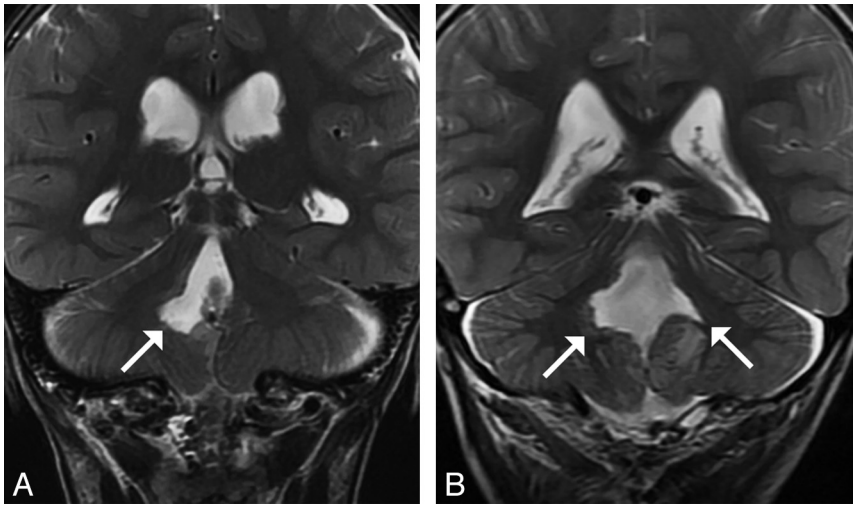

Fig 4. Coronal T2-weighted images in 2 different patients, illustrating unilateral (*A*) and bilateral (*B*) damage to the dentate nuclei (*arrows*).

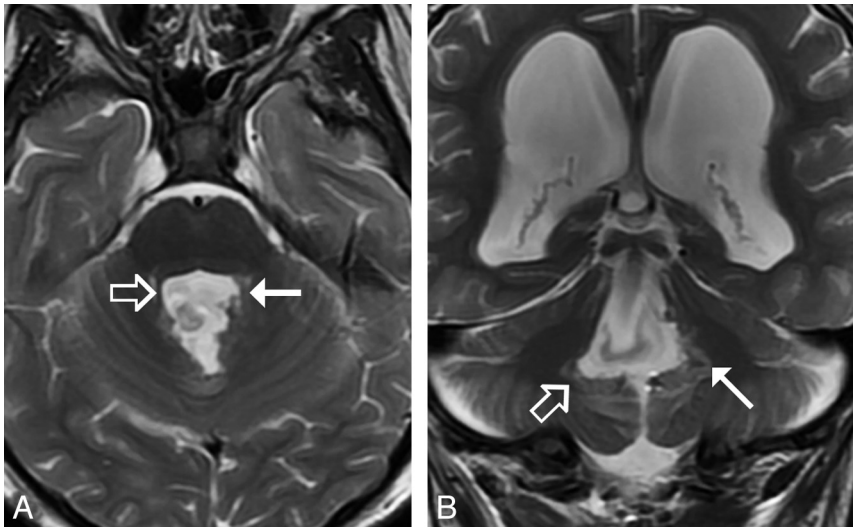

Fig 5. Axial (*A*) and coronal (*B*) T2-weighted images showing obvious damage to the left superior cerebellar peduncle (*solid arrow*) and normal right superior cerebellar peduncle (*open arrow*). The dentate nuclei were more challenging to assess. Damage to the left side (*solid arrow*) was considered definite, whereas damage on the right side (*open arrow*) was considered partial. This was a patient who was believed to have only unilateral damage to the proximal ECP on the basis of anatomic damage analysis, but still went on to have PFS clinically, suggesting that the actual lesion involvement of the dentate nuclei was bilateral.

Regional values of statistical significance ($P < .05$)

	Control Subjects		Cases		
Measure	Mean	SD	Mean	SD	*P* Value
Cerebral blood flow (mL/min/100 g)					
Left frontal polar region, section 5	76.2	29.9	53.3	17.0	.019
Right frontal polar region, section 7	68.5	27.5	46.0	18.0	.041
Right frontal region, section 3	91.1	40.7	57.8	19.6	.037
Right frontal region, section 5	107.9	33.6	76.4	26.0	.023
Right frontal region, section 7	125.9	37.9	83.6	28.6	.025
Left frontal region, section 7	129.3	41.9	86.7	29.9	.023
Right temporal parietal region, section 3	112.9	37.6	84.7	41.4	.023

damage to any component of the pECP during surgery could cause trans-synaptic disruption of "vital" cerebellar input toward the cerebral cortex in areas critical to many basic neurocognitive and executive functions and lead to PFS.

The results of our postoperative anatomic damage pattern analysis suggest that PFS may indeed be caused by disruption of the cerebellocerebral projections because of bilateral damage to the pECP during surgery. Furthermore, in patients with PFS, DSC data showed a trend to global cerebral cortical hypoperfusion with frontal predominance, which was detectable shortly after surgery, and synchronously with the development of clinical manifestations of the syndrome—suggestive

of a peculiar, bilateral crossed cerebellocerebral form of diaschisis.

The phenomenon of reversed crossed cerebrocerebellar diaschisis has also been described previously, though its role has not been advocated in the context of PFS.[14,15] Considering PFS to be a form of diaschisis, one would expect that damage to the pECP would cause a disconnection between the dentate nuclei and its projections to the thalami and cerebral cortex with resultant hypometabolism and hypoperfusion in the affected target areas. As a result, one would see hypoperfusion primarily in the frontal cortical areas and/or in the thalami in patients with PFS with respect to control subjects. Indeed, patients with PFS in our study showed a global trend of hypoperfusion compared with control subjects, with statistically significant differences concentrated within frontal lobe regions. This finding is remarkable in that it correlates with clinical observations of patients with PFS regarding mutism, cognitive impairment, and emotional lability.[1] This would suggest that mutism in PFS is probably a speech apraxia rather than a simple dysarthria, dysphasia, or other cerebellar speech disorder.

From a clinical standpoint, patients who undergo surgery for posterior fossa midline tumors often have some degree of speech impairment localized to the brain stem and/or cerebellum afterward. However, what separates the patients with PFS from the usual patients with postsurgical medulloblastoma with "postoperative speech disorder" is the supratentorial language and apraxic component. This is in addition to dysarthria and ataxic ("scanning") speech that any patient may experience after posterior fossa surgery. In general, apraxias are related to dysfunction of supratentorial cortex, and patients with PFS do have findings beyond mutism per se that are necessarily localized to the cerebrum, such as oromotor apraxia. It is noteworthy that these patients cannot purse lips, pucker, smile, or even open the mouth on command but will do so spontaneously. In other words, they have the necessary muscle strength, innervation, and coordination as evidenced by spontaneous activity, but they do not have the ability to initiate and execute these actions on command, which normally requires higher-order associative functions not within the purview of the cerebellum and/or brain stem.

It is somewhat surprising that measurable perfusion changes were not observed within the thalami (the most robust relay stations along the efferent cerebellar pathways) of patients with PFS, which may have several possible explanations. First, central nervous system connections both to and from the thalamus are extensive. The reduction of activity in 1 pathway (among many) to the thalamus may not have been enough to observe hypoperfusion within the thalamus as a whole. In other words, had there been a difference in thalamic perfusion between patients with PFS and control subjects (at the level of specific nuclei rather than globally), our study may not have been sensitive enough to detect it because we targeted the thalamus in its entirety rather than at the level of individual nuclei.

The implications of our analyses largely coincide with current thinking in the literature regarding both diaschisis and PFS. Patients with PFS in our series experienced bilateral hypoperfusion in cortical areas remote to the site of primary brain damage, without significant asymmetry. This finding supports our theory that PFS is a bilateral form of cerebellocerebral diaschisis. Our analysis of the surgical damage patterns to the pECP supports the current claim that the development of PFS requires bilateral damage to the dentate nuclei and/or its output pathways.[3,4]

We recognize that our results and their interpretation do not provide plausible explanation of the somewhat delayed onset of PFS with regard to surgery and the actual surgical damage to the pECPs. From a theoretic standpoint, diaschisis-related functional changes should take effect immediately after primary damage, and it is unclear what mechanism may delay the onset of the clinical manifestations in PFS. The explanation for the short latent period remains to be elucidated. It is nevertheless remarkable that a recent study showed diaschisis-related hemodynamic changes in cerebrocerebellar diaschisis (evidenced by increased time-to-peak and decreased CBF in the contralateral cerebellar cortex) only in approximately 15% of patients, who were studied within 5 days after the onset of a large supratentorial ischemic stroke,[16] whereas other investigators, including ourselves (unpublished data), performing similar studies at later time points have found measurable perfusion parametric alterations in significantly higher proportions.[7] One may therefore speculate whether diaschisis-related perfusion changes (and their clinical manifestations) are indeed immediate, as it has been suggested in the past, or are somewhat delayed, through a yet poorly understood mechanism. The explanation of the more-or-less reversible nature of PFS is perhaps somewhat more straightforward. It is quite conceivable that with time, compensatory mechanisms develop with use of collateral or accessory neural pathways in line with the widely accepted concept of functional brain plasticity.

We believe that our findings have important clinical significance. Current surgical strategies used in the treatment of tumors of the midline posterior fossa (aiming at achieving maximal tumor resection) make the dentate nuclei (in particular, the hilus), superior cerebellar peduncles, and mesencephalic tegmentum vulnerable to damage. Rightly, possible total tumor removal remains the ultimate objective of the surgical treatment of posterior fossa tumors in general and medulloblastomas in particular. However, we believe that recognition of the potential consequences of bilateral damage to these key structures is important in the preoperative risk assessment of these patients and may help to reduce inadvertent or unnecessary postoperative morbidity. This would imply that PFS may be preventable through understanding the pathomechanism and adjusting surgical approaches. In addition, the ability to use immediate postoperative imaging of patients who have undergone posterior fossa surgery to anticipate the onset of PFS may also be valuable. Because PFS has a delayed onset of a few days to 1 week after surgery, an immediate evaluation of postoperative images could be used as a screening tool to identify patients at risk for PFS. In the future, early identification of such patients may allow prompt institution of targeted rehabilitative measures to limit the clinical impact of PFS. Because diaschisis does not cause early or short-term visible structural changes on anatomic MR images, it has previously been impossible to detect or predict the existence of diaschisis-related changes in the brain from a conventional imaging standpoint. However, as we come to further understand cerebral hemodynamic changes in all forms of di-

aschisis, including PFS, the potential of improving our understanding of the dynamics of diaschisis-related pathophysiologic changes and their clinical correlates becomes more promising.

Because this study was primarily of an exploratory nature, there were some inherent limitations. Specifically, because we wanted to detect any potential differences between patients with PFS and corresponding control subjects, we did not adjust any statistical tests for multiplicity. Therefore, some caution should be taken when interpreting the results of our study because of the large volume of statistical tests. Although significant areas of hypoperfusion within the frontal lobes suggest a disruption of cerebellar efferent signals to key cortical areas (motor, premotor, and prefrontal), we were unable to measure perfusion in these specific cortical areas per se. However, the arbitrary regional parcellation schema was necessary to ensure that the perfusion data for all subjects were processed in the same, exact manner. Finally, an evaluation of bilateral damage in postsurgical images was unable to predict all of the PFS cases in our study. It should be noted, however, that most of the postsurgical MR imaging examinations were performed at outside institutions with techniques that were not standardized and optimized for the visualization of the pECP. The explanation for this lies in that the primary objectives of early postoperative MR imaging studies are to rule out any immediate surgical complications and assess for a significant residual tumor. Under such circumstances, imaging parameters and strategies are usually not optimized for accurate anatomic assessment of specific structures within the pECP. Although definite damage and total lack of damage to these structures were usually easy to recognize, the inclusion of categories such as vasogenic edema and possible/partial damage in our scoring system (even if justified) reflects our difficulties in less straightforward cases during the evaluation process. If the postoperative MR imaging examinations of patients who have undergone posterior fossa surgery were optimized for accurate anatomic delineation of these relatively small structures with high spatial and contrast resolution sequences (eg, T2 and/or FLAIR with 512 matrix, 3-mm sections) and appropriate section orientation, these examinations as a screening tool for surgical damage to the pECP might become more accurate and reliable. The systematic use of diffusion-weighted imaging (unfortunately not available for all of our patients) may be important as well because that technique has the potential to allow for differentiation between vasogenic edema (indicating presumably reversible, transient surgical damage) and cytotoxic edema (believed to be associated with more profound, potentially irreversible damage to affected structures) in cases where complete structural damage is equivocal.

Conclusions

Our data, on the basis of hemodynamic parametric analysis, indicate global functional depression of cerebral cortical activity in patients with PFS, with a predilection to frontal regions. In addition, logistic regression analysis showed that bilateral surgical damage to the pECP is the likely anatomic substrate of PFS. On the basis of these findings, we propose that PFS follows bilateral disruption of cerebellar input to the cerebral cortex because of surgical damage to any structure along the efferent cerebellar pathway and that PFS is likely a bilateral form of reversed cerebrocerebellar diaschisis. Therefore, cerebellar mutism is likely a form of speech apraxia secondary to diaschisis-related dysfunction of the frontal cortex. The trend to global cerebral cortical hypoperfusion in patients with PFS may explain the complex (ie, not limited to cerebellar mutism) neurocognitive disturbances included in PFS.

We believe that the results of our research are significant because they shed new light on both the cause and the pathomechanism of PFS. Our work implies that it is possible to use early postoperative MR imaging as a screening tool for the onset of PFS and that it may be possible to adjust surgical techniques to minimize the risk for the development of PFS without jeopardizing the completeness of tumor removal, whenever possible. Our analysis also indicates that it is possible to use MR perfusion imaging techniques to detect the functional sequelae of PFS and potentially other diaschisis-related diseases as well.

Acknowledgments

The authors thank Dr. Qing Ji for his expertise and efforts in software development as well as his assistance and guidance in the processing and analysis of the MR examinations.

References

1. Robertson PL, Muraszko KM, Holmes EJ, et al. **Incidence and severity of postoperative cerebellar mutism syndrome in children with medulloblastoma: a prospective study by the Children's Oncology Group.** *J Neurosurg* 2006;105:444–51
2. Turgut M. **Transient "cerebellar" mutism.** *Childs Nerv Syst* 1998;14:161–66
3. Kusano Y, Tanaka Y, Takasuna H, et al. **Transient cerebellar mutism caused by bilateral damage to the dentate nuclei after the second posterior fossa surgery—case report.** *J Neurosurg* 2006;104:329–31
4. Koh S, Beckwitt Turkel S, Baram TZ. **Cerebellar mutism in children: report of six cases and potential mechanisms.** *Pediatr Neurol* 1997;16:218–19
5. Nolte J, Sundsten J. *The Human Brain: An Introduction to its Functional Anatomy.* Philadelphia: Mosby; 2009
6. Mariën P, Engelborghs S, Fabbro F, et al. **The lateralized linguistic cerebellum: a review and a new hypothesis.** *Brain Lang* 2001;79:580–600
7. Yamada H, Koshimoto Y, Sadato N, et al. **Crossed cerebellar diaschisis: assessment with dynamic susceptibility contrast MR imaging.** *Radiology* 1999;210:558–62
8. Parkes LM, Rashid W, Chard DT, et al. **Normal cerebral perfusion measurements using arterial spin labeling: Reproducibility, stability, and age and gender effects.** *Magn Reson Med* 2004;51:736–43
9. Van Laere K, Versijpt J, Audenaert K, et al. **Tc-99m-ECD brain perfusion SPET: variability, asymmetry and effects of age and gender in healthy adults.** *Eur J Nucl Med* 2001;28:873–87
10. Ji Q, Glass JO, Reddick WE. **A novel, fast entropy-minimization algorithm for bias field correction in MR images.** *Magn Reson Imag* 2007;25:259–64
11. Reddick WE, Glass JO, Cook EN, et al. **Automated segmentation and classification of multispectral magnetic resonance images of brain using artificial neural networks.** *IEEE Trans Med Imaging* 1997;16:911–18
12. Reddick WE, Glass JO, Langston JW, et al. **Quantitative MRI assessment of leukoencephalopathy.** *Magn Reson Med* 2002;47:912–20
13. Jain JJ, Glass JO, Reddick WE. **Automated arterial input function identification using self organized maps. SPIE International Symposium on Medical Imaging, Image Processing Conference**. 2007;2–17
14. Tecco JM, Wuilmart P, Lasseaux L, et al. **Cerebello-thalamo-cerebral diaschisis: A case report.** *J Neuroimaging* 1998;8:115–16
15. Mariën P, Baillieux H, De Smet HJ, et al. **Cognitive, linguistic and affective disturbances following a right superior cerebellar artery infarction: a case study.** *Cortex* 2009;45:527–36
16. Lin DD, Kleinman JT, Wityk RJ, et al. **Crossed cerebellar diaschisis in acute stroke detected by dynamic susceptibility contrast MR perfusion imaging.** AJNR *Am J Neuroradiol* 2009;30:710–15